

# Initiation structure of oblique detonation waves behind conical shocks

Cite as: Phys. Fluids **29**, 086104 (2017); <https://doi.org/10.1063/1.4999482>

Submitted: 17 April 2017 • Accepted: 08 August 2017 • Published Online: 24 August 2017

 Pengfei Yang, Hoi Dick Ng, Honghui Teng, et al.



View Online



Export Citation



CrossMark

## ARTICLES YOU MAY BE INTERESTED IN

[Numerical study of oblique detonation wave initiation in a stoichiometric hydrogen-air mixture](#)

Physics of Fluids **27**, 096101 (2015); <https://doi.org/10.1063/1.4930986>

[Detonation structures behind oblique shocks](#)

Physics of Fluids **6**, 1600 (1994); <https://doi.org/10.1063/1.868273>

[Numerical study on reflection of an oblique detonation wave on an outward turning wall](#)

Physics of Fluids **32**, 046101 (2020); <https://doi.org/10.1063/5.0001845>

APL Machine Learning

Open, quality research for the networking communities

**Now Open for Submissions**

LEARN MORE

AIP  
Publishing

# Initiation structure of oblique detonation waves behind conical shocks

Pengfei Yang,<sup>1</sup> Hoi Dick Ng,<sup>2</sup> Honghui Teng,<sup>3,a)</sup> and Zonglin Jiang<sup>1</sup>

<sup>1</sup>State Key Laboratory of High Temperature Gas Dynamics, Institute of Mechanics, Chinese Academy of Sciences, Beijing 100190, China

<sup>2</sup>Department of Mechanical and Industrial Engineering, Concordia University, Montreal, Québec H3G 1M8, Canada

<sup>3</sup>Department of Mechanics, School of Aerospace Engineering, Beijing Institute of Technology, Beijing 100081, China

(Received 17 April 2017; accepted 8 August 2017; published online 24 August 2017)

The understanding of oblique detonation dynamics has both inherent basic research value for high-speed compressible reacting flow and propulsion application in hypersonic aerospace systems. In this study, the oblique detonation structures formed by semi-infinite cones are investigated numerically by solving the unsteady, two-dimensional axisymmetric Euler equations with a one-step irreversible Arrhenius reaction model. The present simulation results show that a novel wave structure, featured by two distinct points where there is close-coupling between the shock and combustion front, is depicted when either the cone angle or incident Mach number is reduced. This structure is analyzed by examining the variation of the reaction length scale and comparing the flow field with that of planar, wedge-induced oblique detonations. Further simulations are performed to study the effects of chemical length scale and activation energy, which are both found to influence the formation of this novel structure. The initiation mechanism behind the conical shock is discussed to investigate the interplay between the effect of the Taylor-Maccoll flow, front curvature, and energy releases from the chemical reaction in conical oblique detonations. The observed flow fields are interpreted by means of the energetic limit as in the critical regime for initiation of detonation. *Published by AIP Publishing.* [<http://dx.doi.org/10.1063/1.4999482>]

## I. INTRODUCTION

An oblique detonation wave is a classical problem in gasdynamics that has long been a subject of experimental, analytical, and lately numerical investigations. Its basic research has significant value to the generic knowledge of high-speed compressible reacting flows.<sup>1</sup> In recent years, oblique detonation as an alternative for supersonic combustion has gained significant interest for air-breathing, hypersonic propulsion systems because of its potential to offer greater efficiency.<sup>2-4</sup> This combustion mode has led to the development of Oblique Detonation Wave (ODW) engines and ram accelerators.<sup>5</sup> After several decades of research, however, there remain challenges to stabilize a steady oblique detonation in high-speed, combustible mixtures. Recent efforts have been focusing on a better fundamental understanding of the oblique detonation initiation and instability with the goal of developing workable ODW engines.

In the literature, there have been extensive investigation of oblique detonation waves beginning with the early theoretical studies of steady ODWs initiated from semi-infinite wedges using shock and detonation polars to determine different wave angles, e.g., Gross,<sup>6</sup> Pratt *et al.*,<sup>7</sup> and Ashford and Emanuel.<sup>8</sup> Later studies then focused on the formation structure of ODWs. The pioneering work of Li *et al.*<sup>9,10</sup> presented the first simulations of this structure composed

of a non-reactive oblique shock, an induction region, a set of deflagration waves, and the oblique detonation surface. More recent studies also showed that there exists other type of oblique shock-to-detonation transition structure depending on different chemical and aerodynamic parameters. Unlike the classical structure described in the previous studies<sup>9,11</sup> where the transition occurs abruptly through a multi-wave point connecting the oblique shock and the detonation surface, the transition may occur smoothly from a curved shock.<sup>12-14</sup> From several parametric studies using numerical simulation, fine scale, instability features on the oblique detonation surfaces similar to the unstable frontal structure of normal cellular detonations have been demonstrated.<sup>13,15,16</sup> The evolution of these instabilities on the oblique detonation surfaces becomes also subject of a number of recent investigations.<sup>17-20</sup> The complex, transient structure near the low Mach limit was also demonstrated,<sup>19,21-23</sup> as well as the effects of non-ideal mixing.<sup>24-26</sup> From the viewpoint of propulsion, Sislian *et al.*<sup>27</sup> and Fusina *et al.*<sup>28</sup> focused on near-Chapman Jouguet (CJ), oblique detonation waves and the propulsive performance of ODW engines.

All the aforementioned studies have focused mainly on oblique detonation waves induced by two-dimensional (2D) wedges, usually with a semi-infinite length. However, the experimental studies on oblique detonations are typically performed by projectiles in the tube filled with premixed combustible mixtures, due to the limitation of the shock tunnel.<sup>29</sup> Recent experimental studies of detonation initiation by

<sup>a)</sup> Author to whom correspondence should be addressed: [hhteng@bit.edu.cn](mailto:hhteng@bit.edu.cn)

spherical projectiles included those by Kaneshige and Shepherd,<sup>30</sup> Higgins and Bruckner,<sup>31</sup> Kasahara *et al.*,<sup>32</sup> and Maeda *et al.*<sup>33,34</sup> These studies aimed at identifying the conditions under which a supersonic blunt projectile will initiate a detonation, as well as describing the formation structure and mapping different detonation initiation regimes. Numerical and theoretical investigations have also been performed by Ju *et al.*<sup>35</sup> to determine the detonation initiation boundary based on the kinetic and energy limit concepts.<sup>36,37</sup> The work by Verreault and Higgins<sup>38</sup> looked at the initiation of cone-induced oblique detonations theoretically and experimentally, and five combustion regimes were observed and discussed.

The main differences between the cone-induced and wedge-induced detonations stem from the introduction of the curvature effect and the presence of the Taylor-Maccoll flow.<sup>39</sup> With the presence of front curvature, planar detonations exhibit a velocity deficit due to an increasing flow divergence in the detonation reaction zone.<sup>40</sup> For oblique detonation waves, a velocity deficit results into a decrease of the ODW angle (less than the one without the curvature effect for the wedge-induced case) to reduce the normal velocity component with respect to the ODW. For a hypersonic flow past a semi-infinite cone, the effect of the Taylor-Maccoll flow induces non-uniform temperature and density in the shocked flow field from the cone body to the oblique shock, as opposed to the uniform values behind a planar oblique shock generated by a wedge. Such flow variation is due to the convergence of the streamlines over the cone causing a compression of the gas between the oblique shock and the cone surface.<sup>41</sup> Considering that the detonation initiation occurs in the non-uniform region and the curvature effect on the shock surface, it is not yet clear how such a flow field influences the formation structure of oblique detonations and how planar and conical oblique detonations differ from each other. Both curvatures around the axis of symmetry and the Taylor-Maccoll flow could potentially influence the ignition and failure mechanisms and thus alter the structure of cone-induced oblique detonations as compared to wedge-induced detonations.

Recent investigations on the formation and structure of oblique detonation initiated from semi-infinite wedges and cones are conducted by Verreault *et al.*<sup>39,42</sup> However, their studies focus mainly on the formation and structure of self-sustained Chapman–Jouguet (CJ) ODWs. By comparing the ODW angles obtained from both theoretical analyses with detonation polars and numerical simulations using the method of characteristics and computational fluid dynamics (CFD), they show that an oblique CJ detonation can exist on very low wedge and cone angles (i.e., with deflection angles  $\theta < \theta_{CJ}$  from detonation polars). Their simulations of oblique detonation waves (ODWs) with semi-infinite cones have also elucidated the effects of the front curvature around the cone axis and the Taylor-Maccoll flow. The presence of the curvature is found to allow ODWs to be initiated at angles less than that of a planar CJ oblique detonation. The effect of the Taylor-Maccoll flow is described from their simulation results showing that the temperature on the cone surface is higher than that behind the shock and hence, the chemical induction length along the wall is shorter in the conical configuration. Compression waves

are seen to form closer to the tip as compared with the planar wedge configuration. The reaction front propagates from the cone surface towards the shock surface through a series of streamlines of negative temperature gradients. The resulting decrease of the reaction front intensity leads to a more gradual increase of the wave angle.<sup>39</sup>

In this study, the ODW structures induced by semi-infinite cones are investigated using numerical simulation over a larger range of deflection angles and incident Mach numbers. The present high-resolution numerical results depict a novel ODW formation structure, a similar one revealed also previously by Zhang<sup>43</sup> but with low resolution. In the work by Verreault,<sup>42</sup> an interesting contour plot of reaction progress variables also shows equivalently a similar situation where the ODW angle oscillates with a large and irregular amplitude and a large variation of the induction length behind the shock. It is suggested that the coupling-decoupling phenomenon of the reaction front with the shock is mainly attributed to the shock curvature around the cone axis, but further investigations are required. In this study, the features of this distinct structure are analyzed further in detail, illustrating the interplay between the effect of the Taylor-Maccoll flow, front curvature, and energy releases from the chemical reaction in conical oblique detonations.

## II. PROBLEM FORMULATION AND NUMERICAL METHOD

A schematic of the oblique detonation wave induced by a cone in a combustible gas mixture is shown in Fig. 1. An axisymmetric shock wave is first induced by the cone and subsequently, if the post-shock temperature is sufficiently high, an exothermic reaction is initiated and induces an oblique detonation. For convenience, the coordinate system is rotated to the direction along the cone surface, and simulations based on Cartesian orthogonal uniform grids are carried out in the region enclosed by the dashed line. The computational model is derived from an axisymmetric formulation. It was assumed in the simulation model that the flow is inviscid, as the Reynolds number generally has a relatively high value in the present shock and detonation flow scenarios. In addition, since the primary focus of this study is on the global initiation phenomenon and not on the small scale features like cellular instabilities on

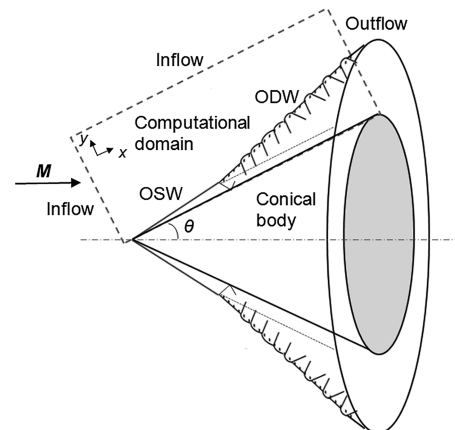


FIG. 1. Schematic of a cone-induced oblique detonation wave.

the oblique detonation surface and details of the compressible turbulent boundary layer interaction, neglecting viscosity seems to be a reasonable assumption. Indeed, previous results<sup>10,12</sup> demonstrate that the viscosity and boundary layer have little effects on the overall structure except changing the boundary layer thickness slightly, and most of the research carried out before is based on the inviscid assumption. Hence, following most of the previous numerical studies,<sup>9,13–23</sup> the present study is also based on the inviscid assumption. Two-dimensional, axisymmetric Euler equations with a one-step irreversible Arrhenius kinetic model are therefore used as the governing equations, i.e.,

$$\frac{\partial \mathbf{U}}{\partial t} + \frac{\partial \mathbf{E}}{\partial x} + \frac{\partial \mathbf{F}}{\partial y} + \frac{\mathbf{AG}}{r} + \mathbf{S} = 0, \quad (1)$$

$$\mathbf{U} = \begin{bmatrix} \rho \\ \rho u \\ \rho v \\ \rho e \\ \rho \lambda \end{bmatrix}, \quad \mathbf{E} = \begin{bmatrix} \rho u \\ \rho u^2 + p \\ \rho uv \\ \rho u(e+p) \\ \rho u \lambda \end{bmatrix}, \quad \mathbf{F} = \begin{bmatrix} \rho v \\ \rho uv \\ \rho v^2 + p \\ \rho v(e+p) \\ \rho v \lambda \end{bmatrix},$$

$$\mathbf{G} = \begin{bmatrix} \rho v' \\ \rho u'v' \\ \rho v'^2 + p \\ \rho v'(e+p) \\ \rho v' \lambda \end{bmatrix}, \quad \mathbf{S} = \begin{bmatrix} 0 \\ 0 \\ 0 \\ 0 \\ \dot{\omega} \end{bmatrix}, \quad (2)$$

with

$$e = \frac{p}{(\gamma-1)\rho} + \frac{1}{2}(u^2 + v^2) - \lambda Q, \quad (3)$$

$$p = \rho T, \quad (4)$$

$$\dot{\omega} = -k\rho(1-\lambda)\exp\left(-\frac{E_a}{T}\right), \quad (5)$$

where  $\rho$ ,  $u$ ,  $v$ ,  $p$ , and  $e$  denote the density, the velocity in the  $x$ - and  $y$ -direction, the pressure, and the total energy, respectively.  $\lambda$  is the reactive progress variable, which varies between 1 (for unburned reactant) and 0 (for product). The mixture is assumed to be ideal and calorically perfect (with a constant specific heat ratio). The parameters  $Q$  and  $E_a$  represent the non-dimensional heat release and activation energy, respectively. These variables have been made dimensionless by reference to the uniform unburned state ahead of the detonation front,

$$\rho = \frac{\tilde{\rho}}{\tilde{\rho}_0}, \quad p = \frac{\tilde{p}}{\tilde{p}_0}, \quad T = \frac{\tilde{T}}{\tilde{T}_0},$$

$$u = \frac{\tilde{u}}{\sqrt{\tilde{R}\tilde{T}_0}}, \quad Q = \frac{\tilde{Q}}{\tilde{R}\tilde{T}_0}, \quad E_a = \frac{\tilde{E}_a}{\tilde{R}\tilde{T}_0}. \quad (6)$$

The pre-exponential factor  $k$  is an arbitrary parameter that merely defines the spatial and temporal scales. It is chosen such that the half reaction zone length  $L_{1/2}$ , i.e., the distance required for half the reactant to be consumed in the steady Zel'dovich-von Neumann-Döring (ZND) wave of the corresponding CJ detonation, is scaled to unit length,  $L_{1/2} = 1.0$ . In the geometric source terms,  $u'$  and  $v'$  represent the velocities along and orthogonal to the inflow direction, expressed as

$$\left. \begin{aligned} u' &= u \cos \theta - v \sin \theta \\ v' &= u \sin \theta + v \cos \theta \\ r &= (x - x_0) \sin \theta + y \cos \theta \end{aligned} \right\}. \quad (7)$$

The rotational transform matrix has the form of

$$\mathbf{A} = \begin{bmatrix} 1 & 0 & 0 & 0 & 0 \\ 0 & \cos \theta & \sin \theta & 0 & 0 \\ 0 & -\sin \theta & \cos \theta & 0 & 0 \\ 0 & 0 & 0 & 1 & 0 \\ 0 & 0 & 0 & 0 & 1 \end{bmatrix}. \quad (8)$$

The governing equations are numerically solved using the MUSCL-Hancock scheme with Strang's splitting. As one second-order extension to Godunov's first order upwind method by constructing the Riemann problem on the inter-cell boundary, this scheme is made total variation diminishing (TVD) with the use of slope limiter MINBEE. The HLLC solver is chosen for the Riemann problem, see the work of Toro.<sup>44</sup> In this study, the dimensionless parameters are fixed with  $Q = 30$ ,  $E_a = 30$ , and  $\gamma = 1.2$ . These values are decided based on previous studies of both oblique and normal cellular detonations.<sup>19,38,45–48</sup> In this study, the focus is on the initiation structure rather than the unstable oblique detonation surface. The combination of moderate heat-release and activation energy renders the detonation relatively more stable to avoid possible numerical issues and extremely large numerical resolution required to resolve all instability features. In addition, these chosen parameters model qualitatively a stoichiometric mixture of hydrogen/oxygen with 70% argon dilution used experimentally in Refs. 38,42. Inflow conditions are fixed at the free-stream values in both the left and upper boundaries of the domain. Outflow conditions extrapolated from the interior are implemented on the right and lower boundaries before the wedge. Slip boundary conditions are used on the wedge surface, which starts from  $x = 0.1$  on the lower boundary. Initially the whole flow field has uniform density, pressure, and velocities, which are calculated according to the inflow Mach number and wedge angle.

### III. NUMERICAL RESULTS AND DISCUSSION

#### A. Wave structures of conical oblique detonations

Figure 2 shows the structure of conical oblique detonations, with the incident Mach number  $M_{in} = 8$  and different semi-cone angles  $\theta = 40^\circ$ ,  $38^\circ$ ,  $36^\circ$ , and  $34^\circ$ . The choice of angles is based on previous studies such as experiments by Verreault and Higgins.<sup>38</sup> More importantly, the main consideration in this computational study is to generate the flow dynamics sensitive to  $M_{in}$  within the limited computational region. The cone-induced ODW is overdriven, and the overdriven degree is usually defined by  $(M_{in} \sin \beta / M_{CJ})^2$ , where  $\beta$  is the oblique detonation angle and  $M_{CJ}$  is the corresponding CJ detonation. The numerical resolution is 128 grids per  $L_{1/2}$  of the CJ detonation, equivalently about 20 grid points within the induction zone of the overdriven ODW, and total grid numbers of about  $2.5\text{--}3.0 \times 10^6$ . Results show that the oblique detonation initiates at about  $x = 7.0$  in the case of  $\theta = 40^\circ$ , and the oblique detonation angle is higher than the upstream oblique shock angle due to the heat release. The oblique detonation surface extends downstream and becomes eventually unstable with the generation of triple points and cellular instability. This cone-induced oblique detonation structure is the

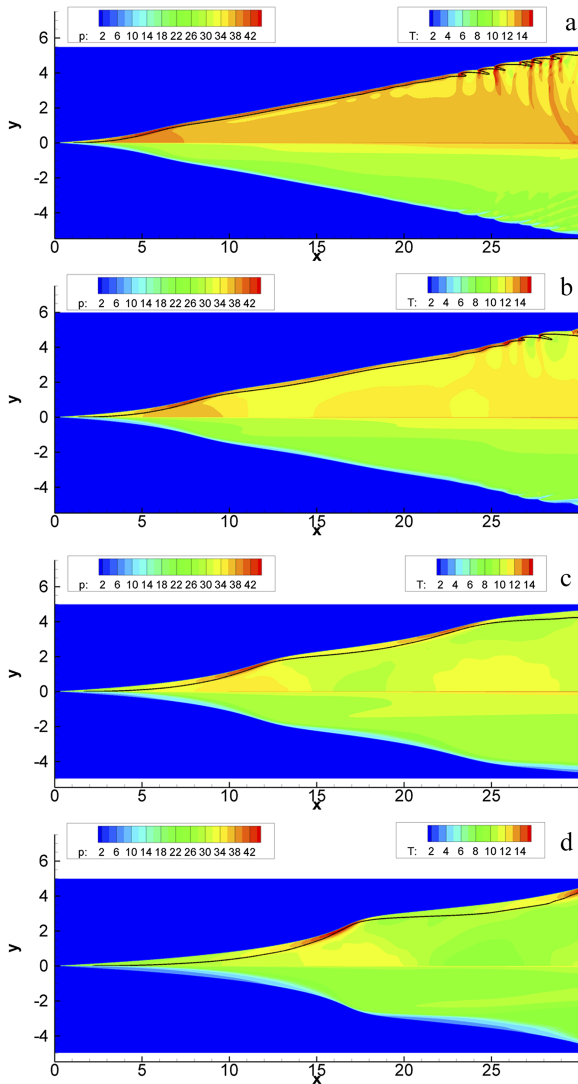


FIG. 2. Pressure (upper, with a black line denotes  $\lambda = 0.5$ ) and temperature (lower) fields of the conical oblique detonation,  $M_{in} = 8$  and  $\theta = 40^\circ$  (a),  $38^\circ$  (b),  $36^\circ$  (c), and  $34^\circ$  (d).

commonly observed one<sup>38,49</sup> and is similar to that induced by a semi-infinite wedge.<sup>16–18</sup> Similar results can be observed by reducing  $\theta$  to  $38^\circ$ , while keeping the same Mach number  $M_{in} = 8$ . However the width between the shock and half reaction zone, denoted by  $\lambda = 0.5$ , becomes large, and its variation along the surface becomes clear.

When the cone angle is further reduced to  $\theta = 36^\circ$ , a novel structure is observed, as shown in Fig. 2(c). Similar to the traditional initiation structure in the above cases, the initial oblique shock and the post-shock compression waves first cause the onset of detonation around  $x = 12$ . Nevertheless, the oblique shock and the reaction zone begin to decouple from each other further downstream, without the immediate formation of smooth or cellular ODW surfaces. The decoupling can be seen by the increase of the post-shock induction zone length, and also the decrease of the oblique surface angle. From the variation of the reaction progress variable  $\lambda$ , the reaction zone is thinner as the ODW angle steepens close to the initiation point and inversely is thicker as the ODW angle decreases due to the decoupling. Another point showing the recoupling

of the oblique shock with the reaction front occurs around  $x = 25$ , but the downstream coupling along the detonation surface tends to become again weak as shown in Fig. 2(c). By further decreasing the angle to  $\theta = 34^\circ$ , a similar structure persists as shown in Fig. 2(d) but the distances for the onset of the first initiation point and between the subsequent ones increase.

This novel structure illustrates the difference of the conical detonation structure from that of planar oblique detonations, and its initiation is attributed to the interplay between the effect of the Taylor-Maccoll flow, shock front curvature, and energy release from the combustion generally. A similar structure has also been reported in the early work by Zhang<sup>43</sup> who referred such observed feature as the “reunion point,” after which an oblique detonation is finally stabilized. It is worth noting that the work by Zhang<sup>43</sup> was done using detailed chemistry with a relatively low numerical resolution and limited domain size. As such, the dynamic mechanism and the detailed characteristics within the flow structure were not probably captured and further studies were necessary.

## B. Verification and validation

In order to ensure the wave structures of conical oblique detonations revealed in Sec. III A are not affected by numerical details such as grid resolution, a verification test is performed. Following our previous works,<sup>19,20</sup> the present simulation uses the coordinates along the cone surface, so the source terms in the governing equations need to be transformed, as shown in Eqs. (7) and (8). To verify the governing equations and the numerical algorithm, the conical shock waves are calculated and compared with the theoretical results, displayed in Fig. 3. In the simulation, all the parameters are the same as the above cases, except setting the heat release  $Q = 0$ . It can be seen that the calculated angles are very close to the theoretical ones, and the difference is around or below  $1^\circ$ . Considering the error in measuring the numerical results, it can be concluded that this set of code is applicable in the conical shock wave simulation.

In order to clarify the effect of numerical resolution on the oblique detonation structure, further simulations with different grid sizes are performed using the same initial and mixture conditions. Figure 4 compares the results of different grid resolutions, i.e., 128 and 256 grids per  $L_{1/2}$ , for the cases with  $M_{in} = 8$ ,  $\theta = 36^\circ$  and  $40^\circ$ . In the case with  $\theta = 36^\circ$  shown in Fig. 4(a)

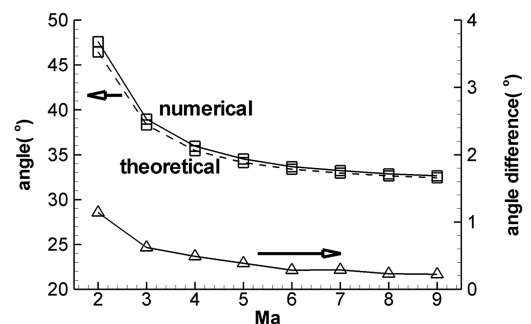


FIG. 3. Theoretical and numerical angles of oblique conical shock waves.

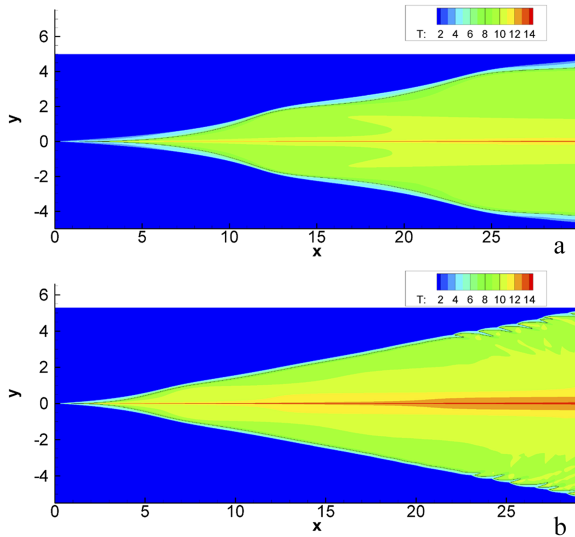


FIG. 4. Temperature field of the conical oblique detonations induced by a cone angle  $\theta = 36^\circ$  (a) and  $\theta = 40^\circ$  (b) with numerical resolutions of 256 (upper) and 128 (lower) grids per  $l_{1/2}$ .

for the novel structure observed, the decoupling reaction fronts on the oblique detonation surfaces are almost the same, and the locations of the two distinct points where there is strong coupling between the oblique shock and reaction front are very close to each other. In the case with  $\theta = 40^\circ$  shown in Fig. 4(b), the temperature fields are almost overlapped except at the cellular detonation surface, and the average distances of transverse waves are close to each other. Our previous study<sup>20</sup> demonstrated that the transverse waves are induced by the upstream weak disturbance between the shock and combustion, and the formation position varies in a certain range, so it is not feasible to get the exact same flow fields. In short, this resolution study confirms that a grid size of 128 grids per  $L_{1/2}$  used in this investigation should provide reasonably converged results of the overall ODW formation structure to support the observation discussed in Sec. III A. However, it is noteworthy that in this numerical investigation the transverse wave generation or the evolution of cellular instabilities on the oblique detonation surface shown in Fig. 4(b) is beyond the scope of this work. In the future investigation, these detailed features should warrant a more thorough and detailed examination of the issue regarding the size of the computational domain and the necessity of increasing the numerical grid resolution.

### C. Feature analysis of conical oblique detonation structures

To investigate the conical oblique detonation features, the streamlines (overlapped on the temperature fields) and the heat release rates of two typical structures are shown in Fig. 5. It is observed that the streamlines in both structures are not parallel to the cone body, but converge together after the oblique shock/detonation surfaces, inducing the relatively high temperature region near the cone body. The streamlines illustrate the effects of the Taylor-Maccoll flow, but it is hard to distinguish the difference of the traditional and novel structures from these. The distribution of the heat release rate is also shown

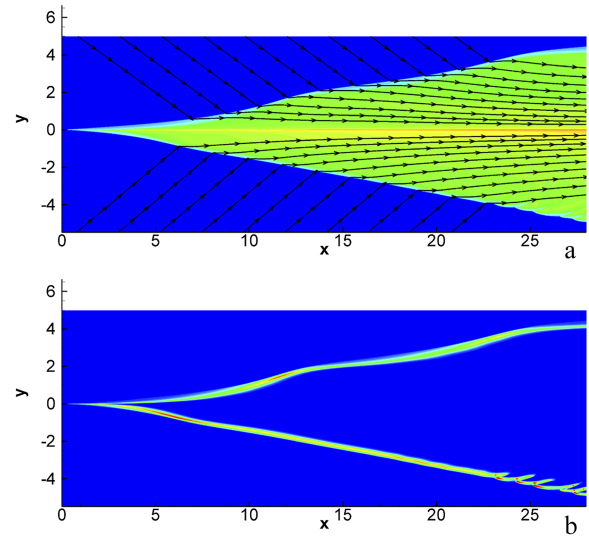


FIG. 5. Temperature field with streamlines (a) and heat release rate (b) of the conical oblique detonation,  $M_m = 8$  and  $\theta = 36^\circ$  (upper) and  $40^\circ$  (lower).

in Fig. 5(b). In the novel structure, the average heat release rate is lower than that of the traditional structure, illustrated by the enlarged thickness of the heat release layer. Furthermore, the heat release oscillation on different surface positions can be seen prominently in the novel structure because the heat release rate of the traditional structure is almost constant on the smooth detonation surface until the transverse waves appear.

The variation of the induction zone length as a function of  $x$ -position is plotted to analyze the conical oblique detonations quantitatively. The induction zone length  $L_{ind}$  is defined as the length between the oblique shock surface and  $\lambda = 0.5$ , along the line paralleled with the  $y$ -axis. Equivalently, it represents the projection of the real induction zone length on the orthogonal direction. Using this approach, the evolution of the induction zone can be magnified considerably.

Figure 6 compares the induction zone lengths  $L_{ind}$  and oblique detonation angles  $\beta$  of two simulation cases. For the traditional structure shown by black lines,  $L_{ind}$  increases first and then decreases to generate one minimum value due to the ODW initiation. Subsequently, another increase appears after  $x = 7$  and reaches its maximum value around  $x = 10$ . It should be noted that this increase is influenced by the flow curvature around the axis, one distinction in the conical flow. In wedge-induced oblique detonations, the second increase will not produce the maximum length beyond the peak of the first increase,<sup>19</sup> and in some cases, there is even no noticeable second hump.<sup>50</sup> Hence, the curvature effect around the axis plays a noticeable role even in the formation of the traditional ODW structure. For the novel decoupling structure, the result given by the red line in Fig. 6(a) clearly shows a more pronounced increase of  $L_{ind}$  generating clearly the second hump, and this significant increase of  $L_{ind}$  indeed indicates the decoupling of the shock and reaction front. Further downstream, the second close-coupling point generates the second trough but is immediately followed by a  $L_{ind}$  increase. A similar trend like  $L_{ind}$  can also be observed on the oblique detonation angles shown in Fig. 6(b). It should be noted that in the traditional

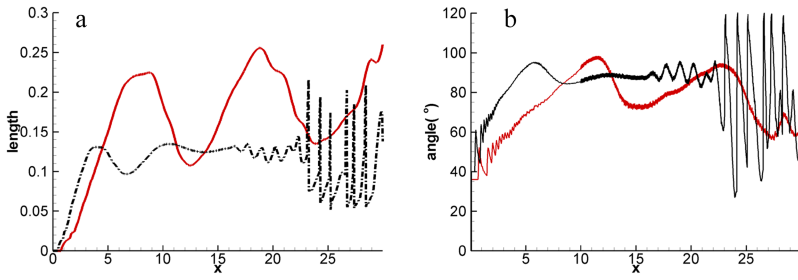


FIG. 6. Induction zone length (a) and oblique detonation angle (b) of the conical oblique detonations,  $M_{in} = 8$  and  $\theta = 36^\circ$  (red lines) and  $40^\circ$  (black lines).

structure, the inherent cellular instabilities manifest starting from around  $x = 20-25$ , introducing the significant length and angle oscillations. Despite these oscillations, the average induction zone length remains small showing the close coupling between the shock and reaction zone in an established oblique detonation wave. Due to the decoupling of the shock and heat release, the oblique shock surface is smooth and the transverse wave generation is suppressed. Generally, the decoupling phenomenon evolves sufficiently, benefiting from the flow expansion due to the front curvature or the characteristics of conical flow, and results into the formation of the novel structure.

To verify that the novel structure is universal and perform further analysis, two additional case groups with  $M_{in} = 9$  and  $M_{in} = 10$  are simulated. With increasing  $M_{in}$  to 9 and keeping the same  $\theta = 36^\circ$ , the simulation result shows the traditional structure rather than the novel one. Only by decreasing  $\theta$ , the traditional structure changes into the novel configuration, and the results with  $\theta = 31^\circ$  are shown in Fig. 7(a). The two distinct points with the shock and reaction front close-coupling are located around  $x = 18$  and  $37$ , respectively. The similar structure with  $M_{in} = 10$  and  $\theta = 27^\circ$  is shown in Fig. 7(b), and both the close-coupling points move downstream further. The induction zone lengths and oblique detonation angles of the case with  $M_{in} = 10$  and  $\theta = 27^\circ$  are again given in Fig. 8. Similar to those shown in Fig. 6, two humps corresponding to the induction zone length increasing can be observed, and also the angle humps with a certain phase shift. These results

demonstrate that the observed structures are not peculiar and represent another class of formation structures in the cone-induced oblique detonations. From the energy point-of-view, reducing the Mach number or deflection angle brings the initiation close to the critical case. The results appear to suggest that the onset of the novel structure with multiple initiation points occurs around the critical condition for successful initiation. Since a simplified one-step Arrhenius chemical kinetic model is used in this study, it is not possible to unanimously define a quantitative threshold for the appearance of this novel structure as in the case to define the critical energy for direct initiation.<sup>51-53</sup> Nevertheless, the appearance of this structure should not be caused by any numerical artifact associated with the use of the simplified one-step chemistry model. As mentioned in Sec. III A, using detailed chemistry but with low numerical resolution, Zhang<sup>43</sup> also observed a similar coupling-decoupling wave structure. Increasing the Mach number or deflection angle, thus the initiation energy, brings these initiation points closer and closer together until the traditional ODW structure is gradually recovered.

The wedge-induced oblique detonations are also simulated and compared with the cone-induced ones shown in Fig. 9. In the 2D planar simulations, the wedge angles are adjusted to generate the same oblique shock angle  $\beta$  as of the conical shock. For example, in the case of  $M_{in} = 10$  and  $\theta = 27^\circ$ ,  $\beta = 31.34^\circ$  is obtained and the corresponding 2D planar wedge angle for this  $\beta$  is calculated to be  $\theta_{2D} = 24.97^\circ$ . Figure 9 shows the 2D planar oblique detonations with  $M_{in} = 8$ ,  $\theta_{2D} = 33.12^\circ$  and  $M_{in} = 10$ ,  $\theta_{2D} = 24.97^\circ$ . Generally, it is observed that the initiation position is located further downstream in the conical case, showing the 2D wedge-induced oblique detonations easier to be triggered in the case of the same oblique

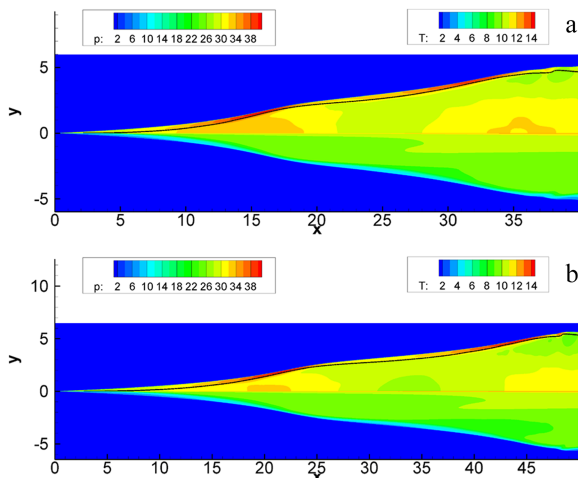


FIG. 7. Pressure (upper, with a black line denotes  $\lambda = 0.5$ ) and temperature (lower) fields of the conical oblique detonation, (a)  $M_{in} = 9$  and  $\theta = 31^\circ$ ; (b)  $M_{in} = 10$  and  $\theta = 27^\circ$ .

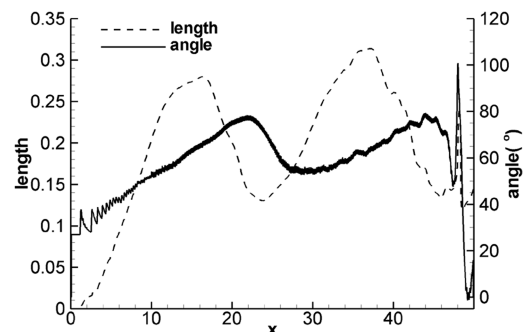


FIG. 8. Induction zone length (dashed line) and oblique detonation angle (full line) of the conical oblique detonation,  $M_{in} = 10$  and  $\theta = 27^\circ$ .

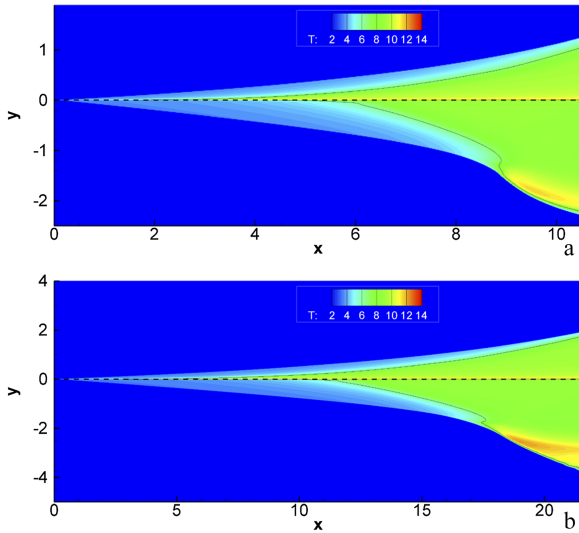


FIG. 9. Temperature field of the conical (upper) and planar (lower) oblique detonations with the same shock deflection angle, (a)  $M_{in} = 8$ ,  $\theta = 36^\circ$ ; (b)  $M_{in} = 10$ ,  $\theta = 27^\circ$ .

shock angle. In detail, these numerical results demonstrate that for the axisymmetric configuration, the heat release starts first at the wall near the cone tip, but its coupling with the shock takes a longer process to form the ODW. Contrarily, the heat release of the 2D planar case starts downstream, but its subsequent coupling with the shock is more rapid. The difference in the heat release process can be readily explained because the temperature and density near the cone wall are about 30% higher than those near the wedge due to the effect of the Taylor-Maccoll flow. On the other hand, the fact that the coupling between the shock and heat release is more difficult to achieve in the conical case demonstrates that the curvature effect plays a more dominant role in the conical oblique detonation initiation. Generally, the curvature can overcompensate the high density and temperature in the shocked gas, inducing the formation of the novel structure with multiple close-coupling re-initiation points in the detonation flow field.

#### D. Discussion of the initiation mechanism

From the above discussion, the curvature effect is crucial in the formation of conical oblique detonation, and the flow divergence can influence the reaction heat release and its subsequent coupling with the oblique shock for the onset of detonation. The heat release rate of the chemical reaction model is controlled by both the pre-exponential factor  $k$  and the activation energy  $E_a$  of the combustible mixture; therefore additional simulations are performed to elucidate the curvature and heat release coupling by varying these two parameters. The pre-exponential factor  $k$  is varied to change the half reaction zone length  $L_{1/2}$ , whose results are shown in Fig. 10. Given the same  $E_a = 30$ , the case with  $L_{1/2} = 0.8$  is shown in Fig. 10(a), and similarly, the case with  $L_{1/2} = 1.2$  is shown in Fig. 10(b). Obviously both the pressure and the temperature are essentially the same, except the different coordinate scales. In other words, the flow fields are self-similar when changing the length scale by adjusting  $k$ . However, the flow

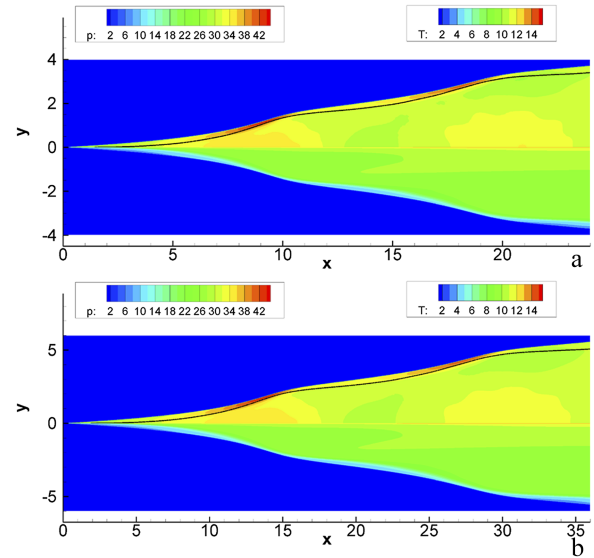


FIG. 10. Pressure (upper, with a black line denotes  $\lambda = 0.5$ ) and temperature (lower) fields of the conical oblique detonation,  $M_{in} = 8$  and  $\theta = 36^\circ$ , (a)  $L_{1/2} = 0.8$ ; (b)  $L_{1/2} = 1.2$ .

fields are different when  $E_a$  is varied, as shown in Fig. 11. In these two cases, the pre-exponential factor  $k$  and the activation energy  $E_a$  are adjusted together to keep the half reaction zone length  $L_{1/2} = 1.0$ . The lower value of  $E_a$  weakens the characteristics of the novel structure, while higher  $E_a$  tends to enhance it. Furthermore, the close-coupling points move upstream when  $E_a$  increases, although  $L_{1/2}$  is kept the same.

The numerical results above demonstrate that the initiation is influenced by the heat release process; thus the corresponding ZND structures are plotted in Fig. 12 for further analysis. With the same  $E_a$  while varying the heat release rate by  $k$ , indeed it can be re-scaled that the ZND structures have similar pressure and temperature profiles in Fig. 12(a). This

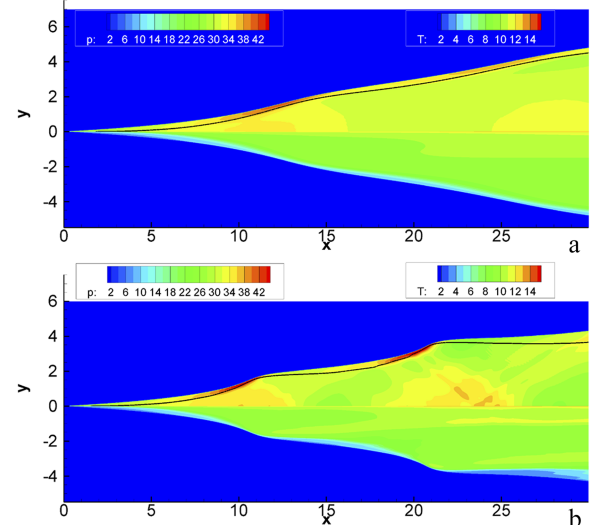


FIG. 11. Pressure (upper, with a black line denotes  $\lambda = 0.5$ ) and temperature (lower) fields of the conical oblique detonation,  $M_{in} = 8$  and  $\theta = 36^\circ$ , (a)  $E_a = 28$ ; (b)  $E_a = 32$ .



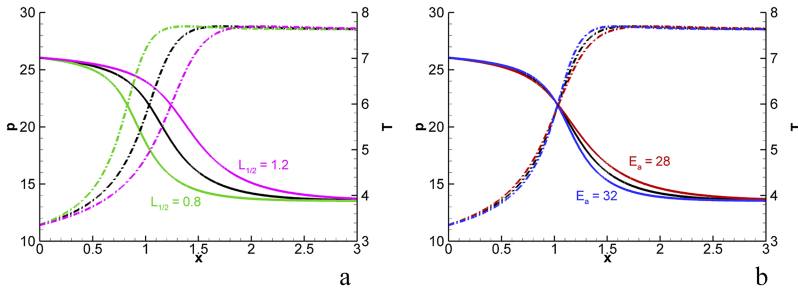


FIG. 12. ZND structure of 1D detonation with different length scales and activation energies.

agrees with the observation on the conical detonation initiation structures, but the scenario becomes more complicated when  $E_a$  changes. In the case of high  $E_a$ , the heat release curve becomes steep as shown in Fig. 12(b), inducing the more unstable detonations studied widely before.<sup>40</sup> In the conical oblique detonations, the steep heat release curve favors the formation of the novel structure, a mechanism equivalent to the pulsating instability of normal detonations. Nevertheless, the one-step irreversible Arrhenius kinetic model has only one interior length scale  $L_{1/2}$ , bringing much difficulty on further analysis. There is no clear definition of the induction zone and heat release zone, thus lacking a chemical “cut-off” mechanism. It is therefore hard to ascertain whether the observed multiple initiation points would be suppressed causing the detonation failure. However again, in the previous study based on the detailed chemistry model by Zhang *et al.*,<sup>43</sup> similar phenomena are also observed, demonstrating that this novel structure is indeed independent of the chemistry model. Generally these results illustrate that the length scale, such as the half reaction zone length  $L_{1/2}$ , decides the initiation position, and the structure is primarily sensitive to the activation energy. For future studies, it is thus recommended to revisit the same problem with a more complex chemical reaction model to quantify the temperature sensitivity of the reaction zone on the initiation structure of conical oblique detonations.

Interestingly, it is worth noting that the flow dynamics observed in this novel structure is comparable to that of the instability regime (or the large disturbance regime) for detonation initiation by blunt projectiles.<sup>54</sup> The combustion front is coupled to the shock in front of the conical projectile and subsequently decoupled several projectile diameters downstream. The present novel structure induced by a semi-infinite cone shows a similar complex interaction between shock-induced combustion and quenching detonation waves with a decoupled zig-zag reaction surface that resembles the flow field behavior of the large disturbance regime about the critical detonation initiation by a blunt projectile.

Lastly, it is worth to re-iterate that the present phenomenon can perhaps also be explained by the energy interpretation, equivalent to the conical projectile problem where the combustion instability regime is generally observed along the energetic limit at increasing cone angle.<sup>38</sup> Such explanation is related to the blast or piston initiation problem of a cylindrical detonation and the observed dynamics is thus governed by the amount of work done to the gas by the cone or the energy deposited given by the pressure drag behind

the initial conical shock. For the direct initiation of a cylindrical or spherical detonation where there is the presence of a curvature term, the simulations by Eckett *et al.*<sup>52</sup> and also by Ng and Lee<sup>53</sup> show that the initiation behavior is more complex. For a range of source energy, despite the successful first onset of the detonation and sometimes a second re-initiation explosion, the detonation can eventually quench again. The dynamics of the cone-induced oblique detonation formation depicted in Figs. 2 and 7 indeed show similar features. For the traditional formation structure, the wave angle oscillates about the steady-state ODW angle as predicted by the theoretical calculation for the given conditions. While for the case of the novel structure as for the near-critical regime of initiation, the detonation first initiates and then approaches failure with subsequently another re-initiation evolution.

#### IV. CONCLUSION

The oblique detonation wave structures induced by semi-infinite cones are investigated numerically using a one-step, irreversible, Arrhenius reaction kinetic model. The present numerical study shows that at large cone angle and incident Mach number, the traditional ODW structure is recovered with the characteristics similar to that of wedge-induced oblique detonations. For the case of low incident Mach number or cone angle, the present numerical results depict a novel formation structure of oblique detonation. In this structure, the strong coupling between the shock and combustion front can be observed at two distinct points. The downstream flow field is characterized by the decoupled shock and reaction front, free of any cellular structure on the shock surface. The formation mechanism of this novel structure is examined by examining the variation of induction reaction zone lengths and surface angles and comparing the flow characteristics with that of planar, wedge-induced oblique detonations. The curvature effect and the non-uniformity of the shocked gas with higher temperature and density derived from the Taylor-Maccoll flow are two additional features to conical ODW. The former is found to be more dominated for the flow of the conical oblique detonations and results into the formation of the novel structure observed in this study. By varying the two chemical parameters of the one-step Arrhenius kinetic model, namely, the pre-exponential factor  $k$  controlling the chemical length scale and the activation energy  $E_a$ , it is found that a steeper heat release curve favors the formation of the novel structure. In other words, the novel structure is influenced dominantly by the temperature

sensitivity of the chemical reaction governed by the activation energy  $E_a$ .

It remains to be determined whether the dynamics of initiation and failure observed in the novel structure is a repeatable process or will there be multiple reunion points coupling again the reaction with the shock and re-establishing the oblique detonation. The answer of this question will require further research and a significantly large computational domain which is not currently admissible with our computing capability. In addition, due to the similar feature of multi-initiation or reunion points as observed by Zhang,<sup>43</sup> the present novel formation structure should not be an artifact of the one-step Arrhenius chemical kinetic model. Nevertheless, high-resolution numerical simulations with realistic thermochemistry would be again desirable in the future study to shed more light on the effect of chemistry on this novel formation structure of conical oblique detonations.

## ACKNOWLEDGMENTS

The research is supported by The National Natural Science Foundation of China NSFC (Nos. 91641130, 11372333, and 51376165), and The Natural Sciences and Engineering Research Council of Canada (NSERC).

- 1 J. M. Powers, "Oblique detonations: Theory and propulsion applications," in *Combustion in High-Speed Flows* (Kluwer Academic Publishers, 1994), pp. 345–371.
- 2 G. P. Menes, H. G. Adelman, J. L. Cambier, and J. V. Bowles, "Wave combustors for trans-atmospheric vehicles," *J. Propul. Power* **8**, 709–713 (1992).
- 3 G. D. Roy, S. M. Frolov, A. A. Borisov, and D. W. Netzer, "Pulse detonation propulsion: Challenges, current status, and future perspective," *Prog. Energy Combust. Sci.* **30**, 545–672 (2004).
- 4 P. Wolański, "Detonation propulsion," *Proc. Combust. Inst.* **34**, 125–158 (2013).
- 5 M. A. Nettleton, "The applications of unsteady, multi-dimensional studies of detonation waves to ram accelerators," *Shock Waves* **10**, 9–22 (2000).
- 6 R. A. Gross, "Oblique detonation waves," *AIAA J.* **1**, 1225–1227 (1963).
- 7 D. T. Pratt, J. W. Humphrey, and D. E. Glenn, "Morphology of standing oblique detonation waves," *J. Propul. Power* **7**, 837–845 (1991).
- 8 S. A. Ashford and G. Emanuel, "Wave angle for oblique detonation waves," *Shock Waves* **3**, 327–329 (1994).
- 9 C. Li, K. Kailasanath, and E. S. Oran, "Detonation structures behind oblique shocks," *Phys. Fluids* **6**, 1600–1611 (1994).
- 10 C. Li, K. Kailasanath, and E. S. Oran, "Effects of boundary layers on oblique-detonation structures," AIAA Paper No. 93-0450, 1993.
- 11 C. Viguier, L. F. Figueira da Silva, D. Desbordes, and B. Deshaies, "Onset of oblique detonation waves: Comparison between experimental and numerical results for hydrogen-air mixtures," *Symp. (Int.) Combust.* **26**, 3023–3031 (1997).
- 12 L. F. Figueira Da Silva and B. Deshaies, "Stabilization of an oblique detonation wave by a wedge: A parametric numerical study," *Combust. Flame* **121**, 152–166 (2000).
- 13 M. V. Papalexandris, "Numerical study of wedge-induced detonations," *Combust. Flame* **120**, 526–538 (2000).
- 14 H. H. Teng and Z. L. Jiang, "On the transition pattern of the oblique detonation structure," *J. Fluid Mech.* **713**, 659–669 (2012).
- 15 M. J. Grismer and J. M. Powers, "Numerical predictions of oblique detonation stability boundaries," *Shock Waves* **6**, 147–156 (1996).
- 16 J. Y. Choi, D. W. Kim, I. S. Jeung, F. Ma, and V. Yang, "Cell-like structure of unstable oblique detonation wave from high-resolution numerical simulation," *Proc. Combust. Inst.* **31**, 2473–2480 (2007).
- 17 M. Y. Gui, B. C. Fan, and G. Dong, "Periodic oscillation and fine structure of wedge induced oblique detonation waves," *Acta Mech. Sin.* **27**, 922–928 (2011).
- 18 J. Verreault, A. J. Higgins, and R. A. Stowe, "Formation of transverse waves in oblique detonations," *Proc. Combust. Inst.* **34**, 1913–1920 (2013).
- 19 H. H. Teng, Z. L. Jiang, and H. D. Ng, "Numerical study on unstable surfaces of oblique detonations," *J. Fluid Mech.* **744**, 111–128 (2014).
- 20 H. H. Teng, H. D. Ng, K. Li, C. T. Luo, and Z. L. Jiang, "Evolution of cellular structure on oblique detonation surfaces," *Combust. Flame* **162**, 470–477 (2015).
- 21 J. Y. Choi, E. J. Shin, and I. S. Jeung, "Unstable combustion induced by oblique shock waves at the non-attaching condition of the oblique detonation wave," *Proc. Combust. Inst.* **32**, 2387–2396 (2009).
- 22 Y. Liu, D. Wu, S. B. Yao, and J. P. Wang, "Analytical and numerical investigations of wedge-induced oblique detonation waves at low inflow Mach number," *Combust. Sci. Technol.* **187**, 843–856 (2015).
- 23 Y. Liu, Y. S. Liu, D. Wu, and J. P. Wang, "Structure of an oblique detonation wave induced by a wedge," *Shock Waves* **26**, 161–168 (2015).
- 24 J. L. Cambier, H. Adelman, and G. P. Menes, "Numerical simulations of an oblique detonation wave engine," *J. Propul. Power* **6**, 315–323 (1990).
- 25 V. V. Vlasenko and V. A. Sabel'nikov, "Numerical simulation of inviscid flows with hydrogen combustion behind shock waves and in detonation waves," *Combust., Explos. Shock Waves* **31**, 376–389 (1995).
- 26 Y. N. Zhang, J. S. Gong, and T. Wang, "Numerical study on initiation of oblique detonations in H<sub>2</sub>-air mixtures with various equivalence ratios," *Aerosp. Sci. Technol.* **49**, 130–134 (2016).
- 27 J. P. Sislian, R. Dubeout, H. Schirmer, and J. Schumacher, "Propulsive performance of hypersonic oblique detonation wave and shock-induced combustion ramjets," *J. Propul. Power* **17**, 599–604 (2001).
- 28 G. Fusina, J. P. Sislian, and B. Parent, "Formation and stability of near Chapman Jouguet standing oblique detonation waves," *AIAA J.* **43**, 1591–1604 (2005).
- 29 H. F. Lehr, "Experiments on shock-induced combustion," *Astronaut. Acta* **17**, 589–597 (1972).
- 30 M. J. Kaneshige and J. E. Shepherd, "Oblique detonation stabilized on a hypervelocity projectile," *Symp. (Int.) Combust.* **26**, 3015–3022 (1996).
- 31 A. J. Higgins and A. P. Bruckner, "Experimental investigation of detonation initiation by hypervelocity blunt projectiles," in 34th Aerospace Sciences Meeting and Exhibit, Aerospace Sciences Meetings, 1996.
- 32 J. Kasahara, T. Arai, S. Chiba, K. Takazawa, Y. Tanahashi, and A. Matsuo, "Criticality for stabilized oblique detonation waves around spherical bodies in acetylene/oxygen/krypton mixtures," *Proc. Combust. Inst.* **29**, 2817–2824 (2002).
- 33 S. Maeda, J. Kasahara, and A. Matsuo, "Oblique detonation wave stability around a spherical projectile by a high time resolution optical observation," *Combust. Flame* **159**, 887–896 (2012).
- 34 S. Maeda, S. Sumiya, J. Kasahara, and A. Matsuo, "Initiation and sustaining mechanisms of stabilized oblique detonation waves around projectiles," *Proc. Combust. Inst.* **34**, 1973–1980 (2013).
- 35 Y. Ju, G. Masuya, and A. Sasoh, "Numerical and theoretical studies on detonation initiation by a supersonic projectile," *Symp. (Int.) Combust.* **27**, 2225–2231 (1998).
- 36 A. A. Vasiljev, "Initiation of gaseous detonation by a high speed body," *Shock Waves* **3**, 321–326 (1994).
- 37 J. H. S. Lee, "Initiation of detonation by a hypervelocity projectile," *Prog. Astronaut. Aeronaut.* **173**, 293–310 (1997).
- 38 J. Verreault and A. J. Higgins, "Initiation of detonation by conical projectiles," *Proc. Combust. Inst.* **33**, 2311–2318 (2011).
- 39 J. Verreault, A. J. Higgins, and R. A. Stowe, "Formation and structure of steady oblique and conical detonation waves," *AIAA J.* **50**, 1766–1772 (2012).
- 40 J. H. S. Lee, *The Detonation Phenomenon* (Cambridge University Press, NY, 2008).
- 41 G. I. Taylor and J. W. Maccoll, "The air pressure on a cone moving at high speeds. I," *Proc. R. Soc. A* **139**, 278–297 (1933).
- 42 J. Verreault, "Initiation of gaseous detonation by conical projectiles," Ph.D. thesis, McGill University, Canada, 2011.
- 43 F. Y. Zhang, "Simulation of conical oblique detonation waves in hypersonic flow of H<sub>2</sub>-air," M.A.Sc. thesis, University of Toronto, Canada, 2005.
- 44 E. F. Toro, *Riemann Solvers and Numerical Methods for Fluid Dynamics*, 3rd ed. (Springer, 2008).
- 45 A. Bourlioux and A. J. Majda, "Theoretical and numerical structure for unstable two dimensional detonations," *Combust. Flame* **90**, 211–229 (1992).
- 46 H. I. Lee and D. S. Stewart, "Calculation of linear detonation instability: One-dimensional instability of plane detonations," *J. Fluid Mech.* **216**, 103–132 (1990).
- 47 M. Short and D. S. Stewart, "Cellular detonation instability. Part 1. A normal-mode linear analysis," *J. Fluid Mech.* **368**, 229–262 (1998).

- <sup>48</sup>G. J. Sharpe, "Transverse waves in numerical simulations of cellular detonation," *J. Fluid Mech.* **447**, 31–51 (2001).
- <sup>49</sup>P. G. Harris, R. Farinaccio, R. A. Stowe, R. Link, D. Alexander, L. Donahue, J. P. Sisljan, and B. Parent, "Structure of conical oblique detonation waves," in Proceedings of the 44th AIAA/ASME/SAE/ASEE Joint Propulsion Conference and Exhibit, 2008.
- <sup>50</sup>T. Wang, Y. N. Zhang, H. H. Teng, Z. L. Jiang, and H. D. Ng, "Numerical study of oblique detonation wave initiation in a stoichiometric H<sub>2</sub>-air mixture," *Phys. Fluids* **27**, 096101 (2015).
- <sup>51</sup>J. H. S. Lee, and A. J. Higgins, "Comments on criteria for direct initiation of detonation," *Philos. Trans. R. Soc., A* **357**(1764), 3503–3521 (1999).
- <sup>52</sup>C. A. Eckett, J. J. Quirk, and J. E. Shepherd, "The role of unsteadiness in direct initiation of gaseous detonation," *J. Fluid Mech.* **421**, 147–183 (2000).
- <sup>53</sup>H. D. Ng and J. H. S. Lee, "Direct initiation of detonation with a multi-step reaction scheme," *J. Fluid Mech.* **476**, 179–211 (2003).
- <sup>54</sup>J. B. McVey and T. Y. Toong, "Mechanism of instabilities of exothermic hypersonic blunt-body flow," *Combust. Sci. Technol.* **3**, 63–76 (1971).